

Research Article

Biosynthesis of Silver Nanoparticles Using *Chenopodium ambrosioides*

Luis M. Carrillo-López,¹ Hilda A. Zavaleta-Mancera,²
Alfredo Vilchis-Nestor,³ R. Marcos Soto-Hernández,² Jesús Arenas-Alatorre,⁴
Libia I. Trejo-Téllez,⁵ and Fernando Gómez-Merino⁵

¹ Fisiología Vegetal, Colegio de Postgraduados, 56230 Texcoco, MEX, Mexico

² Botánica, Colegio de Postgraduados, 56230 Texcoco, MEX, Mexico

³ Centro Conjunto de Investigación en Química Sustentable, UAEM-UNAM, 50200 Toluca, MEX, Mexico

⁴ Instituto de Física, Universidad Nacional Autónoma de México, 04510 Ciudad de México, DF, Mexico

⁵ Edafología, Colegio de Postgraduados, 56230 Texcoco, MEX, Mexico

Correspondence should be addressed to Hilda A. Zavaleta-Mancera; arazavaleta@colpos.mx

Received 30 July 2014; Revised 12 October 2014; Accepted 12 October 2014; Published 25 November 2014

Academic Editor: Xuping Sun

Copyright © 2014 Luis M. Carrillo-López et al. This is an open access article distributed under the Creative Commons Attribution License, which permits unrestricted use, distribution, and reproduction in any medium, provided the original work is properly cited.

Biosynthesis of silver nanoparticles (AgNPs) was achieved using extract of *Chenopodium ambrosioides* as a reducer and coating agent at room temperature (25°C). Two molar solutions of AgNO₃ (1 mM and 10 mM) and five extract volumes (0.5, 1, 2, 3, and 5 mL) were used to assess quantity, shape, and size of the particles. The UV-Vis spectra gave surface plasmon resonance at 434–436 nm of the NPs synthesized with AgNO₃ 10 mM and all extract volumes tested, showing a direct relationship between extract volumes and quantity of particles formed. In contrast, the concentration of silver ions was related negatively to particle size. The smallest (4.9 ± 3.4 nm) particles were obtained with 1 mL of extract in AgNO₃ 10 mM and the larger amount of particles were obtained with 2 mL and 5 mL of extract. TEM study indicated that the particles were polycrystalline and randomly oriented with a silver structure face centered cubic (fcc) and fourier transform infrared spectroscopy (FTIR) indicated that disappearance of the –OH group band after bioreduction evidences its role in reducing silver ions.

1. Introduction

Structures smaller than 100 nm have unusual optical, chemical, photoelectrochemical, and electronic properties. For example, metallic nanoparticles as catalysts are highly reactive and selective in several types of reactions, such as hydrogenation and dehydrogenation [1]. Nanoparticles are prepared by physical and chemical methods that are not environmentally friendly [2], which include chemical reduction in aqueous and nonaqueous solutions, microemulsion method, ultrasound assisted method, and microwave assisted synthesis. Currently there are nanoparticle synthesis procedures assisted by green chemistry using biological systems such as yeasts, fungi, bacteria, and plant extracts for nanoparticle synthesis. Some studies about biosynthesis of gold and

silver nanoparticles based on plant extracts [3] include the use of *Citrus sinensis* [4], *Gardenia jasminoides* Ellis [1], *Brassica juncea*, *Medicago sativa*, and *Helianthus annuus* [5–7], *Opuntia ficus-indica* [8], *Coriandrum sativum* [9], *Hibiscus rosa sinensis* [10], *Capsicum annum* L. [11], *Ocimum sanctum* and *Vitex negundo* [12, 13], *Chenopodium album* [14], *Avena sativa* [15], and *Tridax procumbens*, *Jatropha curcas*, *Calotropis gigantea*, *Solanum melongena*, *Datura metel*, *Carica papaya*, and *Citrus aurantium* [16].

The phytochemistry of the genus *Chenopodium* has been studied and the compounds reported were: minerals, carbohydrates, aminoacids, nonpolar constituents, proteins, aromatic cytokinins, flavonoids, saponins, terpenes, sterols, alkaloids and vitamins [18]. Particularly in *Chenopodium ambrosioides* the secondary metabolites included: organic

acids, flavones (glycoside), flavonols and their glycosides (kaempferol, quercetin, and isorhamnetin), sterols and phytosterols (avenasterol and spinasterol), monoterpenoids (acyclic such as β -myrcene, *cis*- β -ocimene and its *trans*-isomer, nerol and geraniol, and citronellyl acetate; monocyclic such as limonene, α -terpinene and its γ -isomer, α -terpinolene, β -phellandrene, *p*-cymene, carvacrol, thymol, *trans*-pinocarveol and α -terpineol, carvone, pinocarvone, piperitone and its acetates, and ascaridole; and bicyclic such as chanopanone), sesquiterpenoids (β -caryophyllene and γ -curcumene), and carotenoids (α -carotene and β -carotene) [17].

Chenopodium ambrosioides, commonly known in Mexico as “epazote,” is a native aromatic herb, which has a culinary and medicinal use: flavor beans and tortilla dishes. It is also used as anthelmintic, and some of its chemical compounds attack certain lines of cancer [18]. Extract from *C. ambrosioides* has antioxidant effect and can be applied in stabilizing unsaturated compounds in food and pharmaceuticals [17]. The essential oil of *C. ambrosioides* has strong antioxidant activity, it is rich in *p*-cymene (25.4%), (*Z*)-ascaridole (44.4%), and (*E*)-ascaridole (30.2%), and it shows activities against (1) microbes, *Helicobacter pylori*, which cause peptic ulcers and gastritis; (2) fungi causing postharvest deterioration such as *Aspergillum flavus*, *A. glaucus*, *A. niger*, *A. ochraceus*, *Colletotrichum ochraceous*, *C. gloeosporioides*, *C. musae*, *Fusarium oxysporum*, and *F. semitectum*; (3) parasites, *Trypanosoma cruzi*, *Leishmania amazonensis*, *Plasmodium falciparum*, and *Ascaris*; and (4) antineoplastic properties for cancer, fibroids, cysts, and cystadenomas [17].

There are studies about the mechanism of nanoparticle formation by plant extracts and a process of rapid reduction, formation, and sintering at room temperature. Synthesis of gold nanotriangles was carried out using extract of *Aloe vera*; only biomolecules with a molecular weight below 3 kDa caused reduction of tetrachloroauric ions, leading to the formation of gold nanotriangles [19]. Nanoparticles fabricating involves boiling the aqueous solutions in order to extract the organic compounds and to synthesize gold and silver nanoparticles at room temperature, without addition of a nanoparticle protector (coating agent) against aggregation, template formation, or accelerators such as ammonia [19].

Few studies have investigated the dynamics of nanoparticles reduction during large periods and performed a statistical analysis of several experiments. This is the first report on biosynthesis of Ag NP using *Chenopodium ambrosioides* extracts as reducing and capping agent, monitored during 168 h and 12 months, under a statistical analysis to demonstrate significant differences between the treatments, leaf extract volumes, and AgNO₃ concentrations.

2. Materials and Methods

2.1. Plant Material and Preparation of Dry Biomass. *Chenopodium ambrosioides* was cultivated in a greenhouse in Texcoco State of Mexico, Mexico (19.52°N, 98.88°W). The seed was obtained from plants growing freely among cultivated chrysanthemum plants (*Dendranthema grandiflora*, Tzeleu, variety Snow Eleonora). Fully expanded leaves were

harvested, extensively washed with deionized water, and dried in an oven at 65°C for 72 h. Dry leaves were grinded in a mortar to pass a 1.0 mm stainless screen (20 mesh) for homogenous particle size.

2.2. Preparation of Plant Extract. About 2 g of ground and sifted dry biomass was boiled in 100 mL of deionized water for 5 min and left to cool at room temperature (25°C) for 1 h. Then the extract was centrifuged twice at 4000 g for 5 min.

2.3. Silver Nanoparticle Synthesis. Aqueous solutions of silver nitrate (AgNO₃) (Sigma-Aldrich, Mexico) were prepared (1 mM and 10 mM) with deionized water. A known volume (0.5, 1, 2, 3, and 5 mL) of leaf extract was added, drop by drop, to 5 mL of 1 mM or 10 mM aqueous solution of silver, shaking continuously, and gauged to 15 mL using deionized water, observing a brownish color, indicating the formation of Ag NPs.

2.4. UV-Vis Spectrophotometry Analysis. Absorbance was measured in the visible ultraviolet range (350–700 nm) in a Lambda 25 spectrophotometer (PerkinElmer) at a resolution of 1 nm every 0.30 min (from 1.0 to 6.0 h) every 2 h (from 6 to 12 h) and at 24, 38, 77, 96, 120, 140, 168, and 384 h. The dynamics of nanoparticles reduction was assessed plotting the maximum absorbance reached (au) at each time of measurement. The factors evaluated were molar concentrations of AgNO₃ (1 mM and 10 mM) and extract volumes (0.5, 1, 2, 3, and 5 mL). Some samples became too concentrated after 2 h of bioreduction and they were diluted 1 : 10 in deionized water.

2.5. Statistical Analysis. Treatments were five volumes of extract (0.5, 1, 2, 3, and 5 mL) and two molar solutions (1 mM and 10 mM) of AgNO₃ for a total of 10 treatments. The experiment was replicated three times, and analysis of variance with SAS System 9.1 was carried out with the data, and mean values were compared with the Tukey test ($P < 0.05$).

2.6. Morphological Characterization with Transmission Electron Microscopy (TEM). Samples for TEM characterization were obtained from AgNPs solution after 168 h of reaction, when the absorbance was stabilized. Copper grids (mesh 200) were coated with collodion (2% in amyl acetate) and carbon; then 4 μ L of the sample was placed on the grid and allow it to dry in a Petri dish. Particles were observed with a transmission electron microscope (JEM-2010 JEOL) operated at 120 kV. Images were analyzed using Image J (Scion Corporation, Version 1.45) software to estimate size distribution of synthesized particles. Crystalline metallic pattern of Ag NPs was confirmed obtaining the selected area electron diffraction patterns (SAED).

2.7. Infrared Analysis before and after Bioreduction. A volume of 5 mL of the synthesized particles in solution (samples) was centrifuged at 6000 g for 10 min to remove any organic residue that did not participate in the stabilization and control of the nanoparticle size as capping (ligands). The pellet was washed twice with 5 mL of deionized water as described above. The resulting suspension was used for infrared analysis

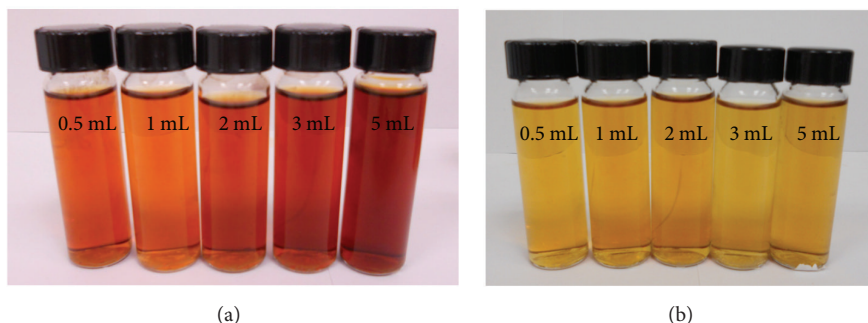


FIGURE 1: Characteristic coloring of silver nanoparticles formed with five volumes of extract and two molar concentrations of AgNO_3 : 10 mM (a) and 1 mM (b).

with an IR-spectrophotometer Platinum equipped with an ATR accessory (Bruker, Tensor 27, Germany). This analysis was performed on the native extract (before AgNPs synthesis) and after bioreduction to identify the organic molecules participating in the synthesis.

3. Results and Discussion

3.1. UV-Vis Spectrophotometry. During NPs synthesis, the solution color changed due to the presence of the “surface plasmon resonance,” an optical characteristic of AgNPs. This phenomenon is related to characteristic surface plasmon spectra of each metal NP [16]. After adding the leaf extract to the 10 mM AgNO_3 solution, the aqueous solutions changed from yellow to yellowish brown; color intensified over time in function of the quantity of extract; 1 mM did not develop this conspicuous color change (Figure 1). The absorption spectrum of the NPs produced with different quantities of *C. ambrosioides* extract is shown in Figure 2. It was found that the quantity of extract affects the absorbance. The highest values were reached with 10 mM AgNO_3 and 5 mL of extract, but using 0.1 mL, the system became stable after 1 h (Figure 2).

This observation is consistent with the report on other species, where silver nanoparticle suspension changed from reddish yellow to deep red increasing the quantities of extract [10, 14, 19].

There is a directly proportional relationship between volume of extract and absorbance value over time; with smaller extract volumes, fewer particles are formed [16]. Figure 2(c) presents high absorbance values for a volume of 5 mL and a 10 mM molar concentration of AgNO_3 ; the corresponding coloring is more intense, and more NPs are synthesized. The larger the volume of extract is, the more intense the color of the colloidal solution of silver nanoparticles is obtained. Insufficient biomolecules for reduction of silver ions lead to formation of few particles, as well as low absorbance values [20].

The lower the molar concentration of silver, the fewer the particles formed. For AgNO_3 1 mM in Figure 2(d), lower absorbance values are observed than in Figure 2(a), using the same volume of extract (1 mL).

TABLE 1: Effect of AgNO_3 concentration on absorbance and wavelength.

| Treatment | Absorbance (a.u.) | Wavelength (nm) | Particle size (nm) |
|-----------|---------------------|--------------------|--------------------|
| 10 mM | 2.7432 ^a | 437.8 ^a | 4.9 ± 3.4 |
| 1 mM | 0.9081 ^b | 429.9 ^b | 5.1 ± 2.3 |

Absorbance and wavelength data are average of 3 experiments. Values in columns with different letters are statistically different ($P < 0.05$). Average size was obtained from 300 particles measured on TEM micrographs.

TABLE 2: Effect of extract volume on absorbance and wavelength of NPs synthesized.

| Treatment | Absorbance (a.u.) | Wavelength (nm) | Particle size (nm) |
|-----------|---------------------|--------------------|--------------------|
| 0.5 mL | 1.1015 ^a | 436.5 ^a | 4.8 ± 2.6 |
| 1 mL | 1.3488 ^b | 434.0 ^b | 4.9 ± 3.4 |
| 2 mL | 2.5529 ^c | 437.9 ^a | 6.2 ± 2.9 |
| 3 mL | 3.4824 ^d | 437.0 ^a | 7.3 ± 2.6 |
| 5 mL | 4.8135 ^e | 432.7 ^c | 8.5 ± 2.8 |

Absorbance and wavelength data are average of 3 experiments. Values in columns with different letters are statistically different ($P < 0.05$). Average size was obtained from 300 particles measured on TEM micrographs.

In *C. ambrosioides* the concentration of AgNO_3 (Table 1) had a significant effect on absorbance and wavelength. The volumes assessed also had a statistically significant effect on absorbance and wavelength (Table 2). Differences between compared treatment means were significant. In *C. album* when the molar concentration of Ag increased, the peak absorbance of the UV-Vis spectrum rose [14], as shown in Table 1.

The surface plasmon resonance (SPR) obtained from the AgNPs synthesized with *C. ambrosioides* (432–437 nm) varies from the SPR reported for *C. album* 460 nm [14]. In *C. album* there was an increase in the absorption of the UV-Vis spectrum as extract volume increased [14]; however, the authors did not follow the dynamics of the synthesis over time as we performed in the experiments with *C. ambrosioides*.

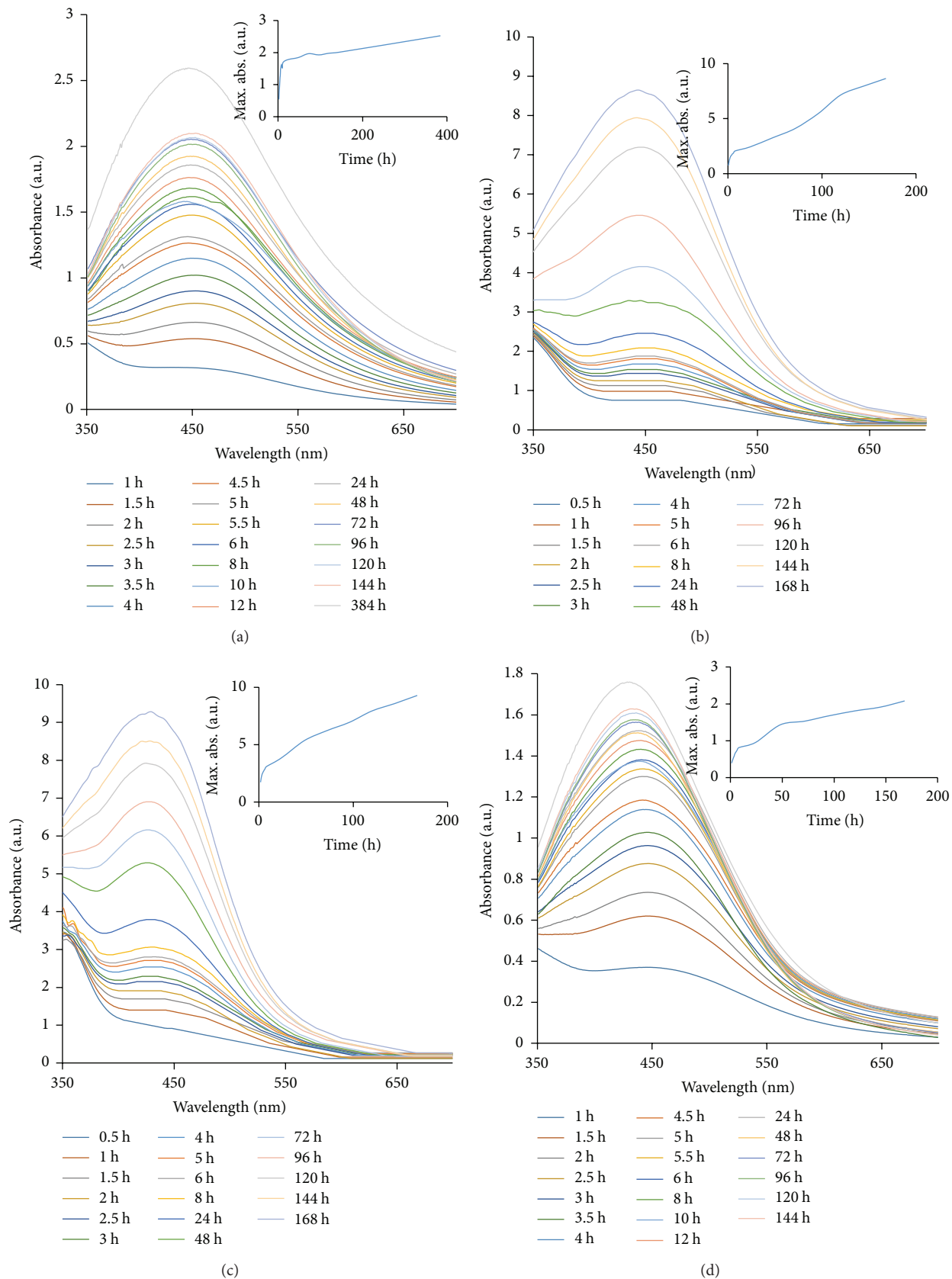


FIGURE 2: UV-Vis spectra of AgNPs synthesized with *Chenopodium ambrosioides* at 25°C. Extract volume of 1 mL (a), 2 mL (b), and 5 mL (c) with 10 mM AgNO_3 , and 1 mL (d) with 1 mM AgNO_3 . Volumes above 1 mL with 1 mM AgNO_3 did not form a characteristic surface plasmon resonance (SPR). The insert corresponds to the stabilization of the system.

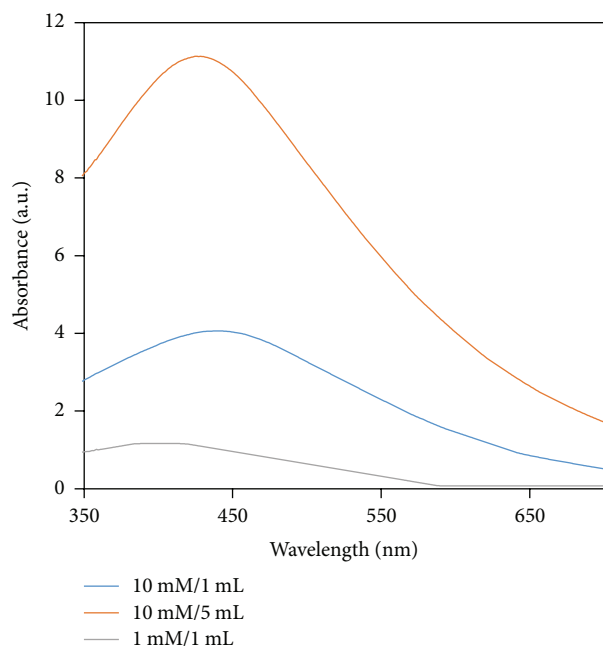


FIGURE 3: UV-Vis absorption spectrum of silver nanoparticles after bioreduction by *Chenopodium ambrosioides* extract at 20°C after 368 days.

Synthesized AgNPs of the present research stored in amber flasks at 20°C were stable after 368 days (one year). NPs produced with 10 mM AgNO₃ and 1 mL of leaf extract showed the best SPR (Figure 3). These results suggested the great stability of the system and the potential of this green protocol.

3.2. TEM Qualitative Assessment. The representative TEM micrographs are presented in Figure 4, showing different magnifications of the particles resulting from the reaction of silver ions and different volumes of *C. ambrosioides* extract. Particles synthesized with 1 and 5 mL in 10 mM AgNO₃ are not uniform in size (Figures 4(a), 4(b), 4(e), and 4(f)). In contrast, particles synthesized with 0.5 mL were smaller (4.9 ± 3.4 nm) and less polydisperse (Figures 4(c), 4(d), and 5(a)). Similar results were obtained for different quantities of *Cinnamomum camphora* biomass, in which the anisotropic nanostructures, such as the nanotriangles or nanoparticles with irregular shapes, were obtained at high quantities of biomass [20]. Figures 4(b), 4(d), and 4(f) show the samples morphology at a higher magnification. In general, with 10 mM the size of the particle increased from 4.9 to 8.5 nm when *C. ambrosioides* extract volume increased from 1 mL to 5 mL. Contrary to our results, in the case of *C. album*, the 10 nm particles were reported at large leaf extract ratio 1:30 (5 mM) of extract [14]. However, studies with *Cinnamomum zeylanicum* indicated that particle size increased from 31 to 100 nm when the quantity of the extract increased [21]. Likewise, at lower concentrations of silver nitrate (1 mM) with 1 mL of bioreducer, smaller particles are obtained, but with less quantity (Figures 4 and 5). In

contrast, an increase in silver ions (from 0.1 to 5 mM AgNO₃) causes an increase in particle sizes. We have obtained similar results with *C. ambrosioides* [14]. Some nanoparticles tend to aggregate in clusters as quasilinear superstructures. Silver nanoparticles that reduce rapidly are polydisperse, while those that reduce more slowly are quasispherical [20]. Similar results were obtained in our study with a smaller volume of *C. ambrosioides* extract; reduction was rapid and polydisperse structures were obtained. Slow reduction, such as that in 3 mL extract and 10 mM AgNO₃ solution, produces uniform particles. Nevertheless, if the quantity of biomass is larger (5 mL), irregular-shaped particles are produced (Figure 4(f)).

In general, particle size can be controlled by changing the volume of the reducing agent (*C. ambrosioides*). Sub-micrometric sized particles 100 to 800 nm were obtained with concentrations above 10% of plant extracts, suggesting that a high quantity of reducing agent causes aggregation of synthesized silver particles, possibly due to the interactions between coating molecules linked to particle surfaces and to secondary reduction processes on the surface of the preformed nucleus [22].

Average particle size decreases by increasing silver nitrate concentration, but so far this result is not well understood. It is believed that particle size and shape are dependent on many factors, such as the type of plant material, type of nanoparticle, temperature at which the reaction takes place, and composition of the reductant extract. According to some studies, 11 minutes is required for the conversion 90% of 0.1 mM silver nitrate into silver nanoparticles and 90 minutes for converting 90% of 2 mM silver nitrate into silver nanoparticles, whereas in our study the conversion reached almost 100% and particle size (0.1 mM) was smaller [22].

The distribution of particle size for the concentrations and volumes used in our study agrees with the results obtained with TEM micrographs (Figure 4).

The smallest particle sizes (4.9 nm and 5.1 nm) were obtained using 1 mL of leaf extract with 10 mM and 1 mM AgNO₃. Using 3 mL and 5 mL of bioreducing the average particle sizes were 7.3 ± 2.6 nm and 8.5 ± 2.8 nm (Figure 5). The increase in size of the particles observed with 3 mL and 5 mL may be due to particle aggregation and mechanisms of secondary reduction [22]. This indicates that the volume of extract has a direct relationship with particle size [15]. In contrast, the concentration of silver nitrate has an indirect relationship with particle size: 5.1 ± 2.3 nm with 1 mM concentration and 4.9 ± 3.4 nm with 10 mM (Figure 4(d)).

The size of the AgNPs obtained using *C. ambrosioides* extracts, for all volumes tested, ranges from 4.9 to 8.5 nm, with low polydispersity. These are considered as small particles (<10 nm) and are smaller than other particles synthesised with different plant species [1, 4, 11, 14, 15, 20, 21] including species of the same genus as *C. album*, whose synthesised particles range from 10 to 40 nm, with large polydispersity [14]. It is well known that small Ag NPs have better catalytic and optical properties and applications than larger particles [20].

It is widely known that the maximum absorbance value tends to change between different wavelength values; it may be due to the relatively large size, polydispersity, and

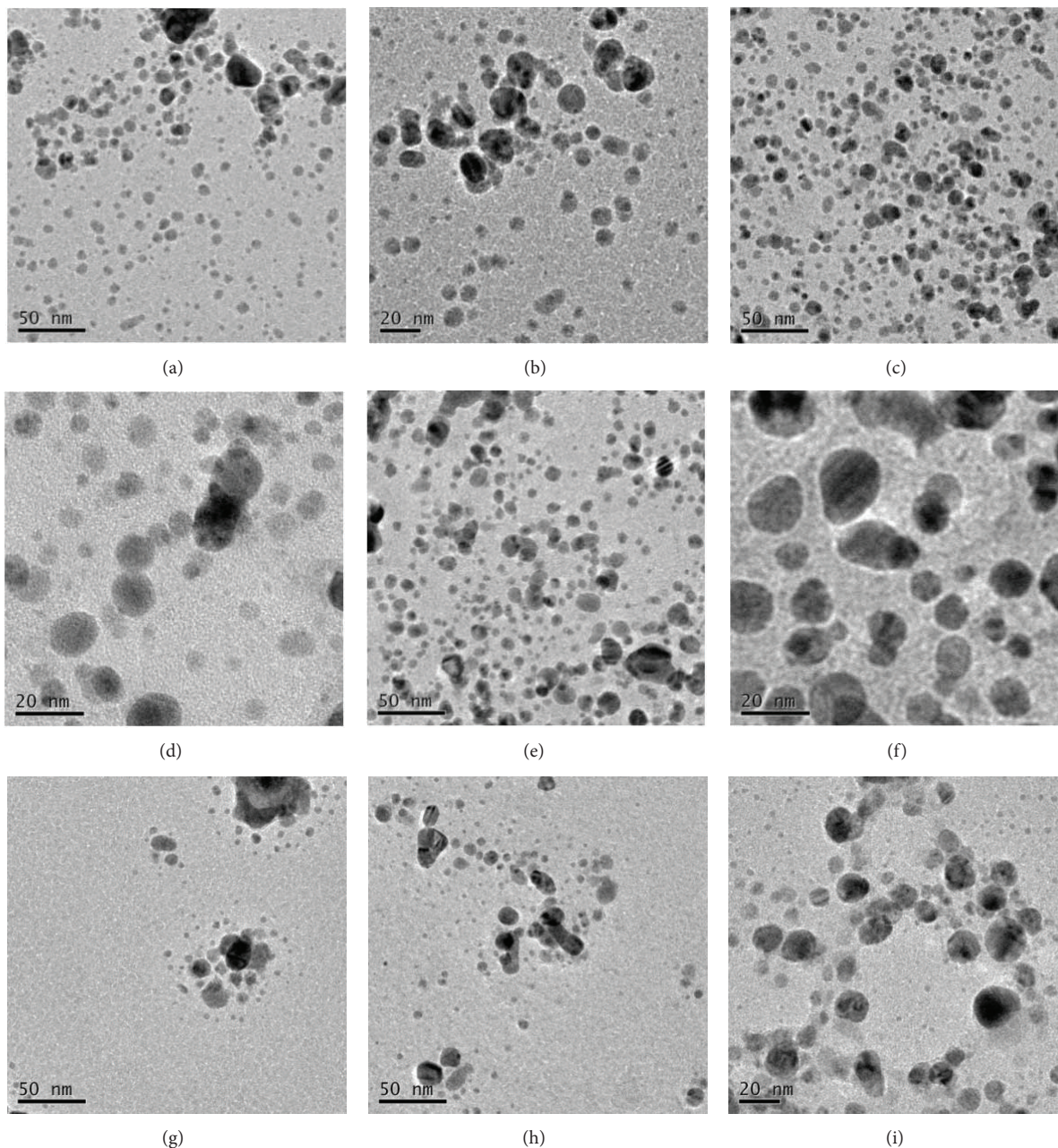


FIGURE 4: Transmission electron micrographs of AgNPs synthesised with *Chenopodium ambrosioides* at 25°C. Extract volume of 1 mL (a-b), 3 mL (c-d), and 5 mL (e-f) exposed to 10 mM AgNO₃. Extract volume of 0.5 mL (g) and 1 mL (h-i) exposed to 1 mM s AgNO₃.

anisotropic shape of the nanoparticles [16]. However a detailed study on the relationship of surface plasmons and metallic NPs characteristics showed the complexity implied behind this quantum phenomenon and the great number of factors which intervene in the characteristics of NPs and how microscopies techniques are suitable to obtain relevant information on nanoparticles morphology [23].

3.3. Selected Area Electron Diffraction Patterns (SAED). All treatments that showed a UV-Vis curve, associated with a

surface plasmon characteristic, presented an electron diffraction pattern of electrons associated with a polycrystalline structure, indicating that the AgNPs synthesized were randomly oriented. The diffraction rings, from inside out, can be indexed with planes (111), (200), (220), and (311), respectively (Figure 6), corresponding to the Ag crystalline phase (JCPDS 04/0784).

3.4. IR Formation Mechanism. The infrared absorption spectrum of aqueous extracts of *C. ambrosioides* before and after

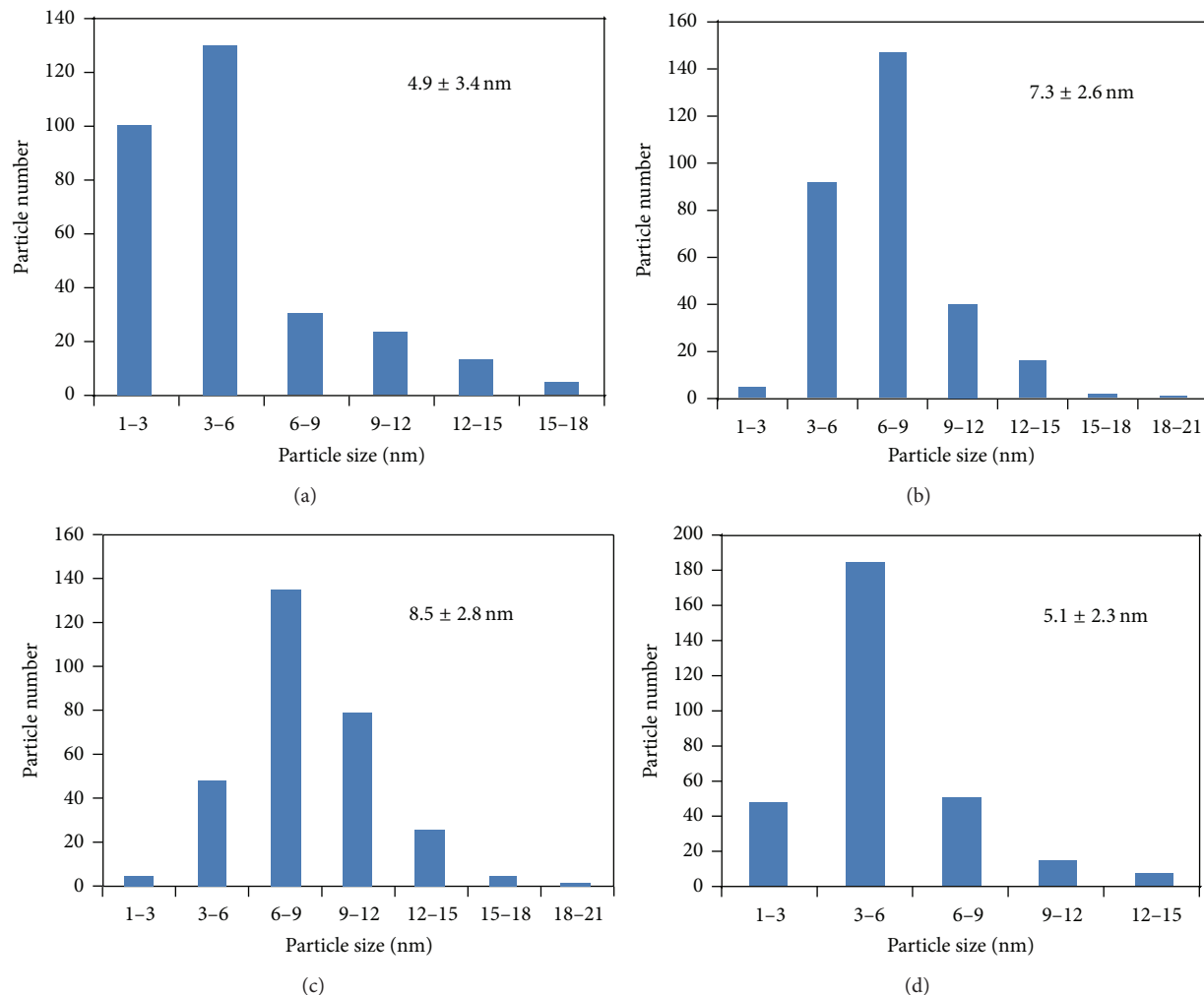


FIGURE 5: Histograms of size distribution of AgNPs synthesized with *Chenopodium ambrosioides* at 25°C. Extract volume of 1 mL (a), 3 mL (b), and 5 mL (c) with 10 mM AgNO₃, and 1 mL (d) exposed to 1 mM AgNO₃. The insert corresponds to mean \pm SD of size particle.

bioreduction provides information about chemical change of the functional groups of the biomolecules associated with the reduction of AgNPs (Figure 7).

In the IR spectrum the line (A) has transmittance band in 3343 cm^{-1} , which is associated with the $-\text{OH}$ stretch vibration and the deformation of $\text{C}-\text{O}-\text{H}$ in phenols (Figure 7). The line (B) represents an IR absorption spectrum after bioreduction; here the signal 3343 disappears, probably due to the reduction of the Ag^+ ions. The increase of transmittance band in 1327 cm^{-1} was associated with the $-\text{COO}$ group, which possibly participated in the stabilization of nanoparticles. The band appearing after bioreduction in 774 cm^{-1} was associated with $-\text{CH}$ in substituted benzenes linked to carboxylate groups.

Phytochemical studies on extracts of *C. ambrosioides* showed that this species possesses large quantities of biomolecules with functional groups $-\text{OH}$ such as terpenoids (*trans*-diol, α -terpineol, monoterpene hydroperoxides, and apiol) and phenolics (flavoglycoside and isorhamnetin), compounds with a well-recognized antioxidant potential [17]. Bioreduction studies in other species have reported the

participation of carbonyl groups in the AgNPs reduction process [3, 9, 10, 17]. Therefore we propose that the terpenoids and flavonoid were the main responsible molecules of the reduction of AgNPs. The presence of carboxylates has been demonstrated, in other systems, showing that they work as stabilizing agents controlling the shape of the particles [14, 23].

Other hypotheses propose that $-\text{OH}$ groups participate in the reduction process, oxidizing $-\text{OH}$ groups to carbonyl groups, and carbonyl and carboxylate groups are involved in the stabilization of particles [20, 23].

Besides, there is contribution of polyols, such as flavones, terpenoids, and polysaccharides, in the biomass [20]. In the case of *C. ambrosioides*, the disappearance of the $-\text{OH}$ group 3343 band after bioreduction evidences that this functional group is mainly responsible for reducing silver ions.

4. Conclusions

This is the first study on the synthesis of AgNPs using aqueous extract of *Chenopodium ambrosioides*, an arvense Mexican

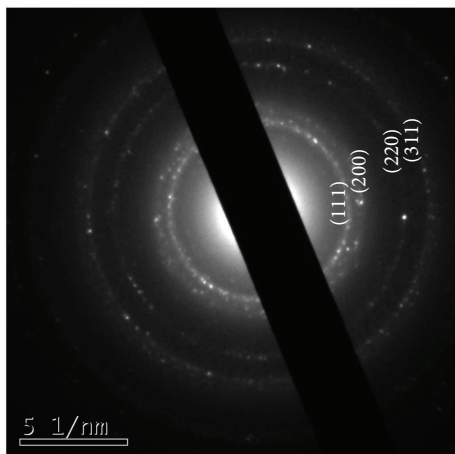


FIGURE 6: Diffraction pattern of electrons corresponding to Ag crystalline phase.

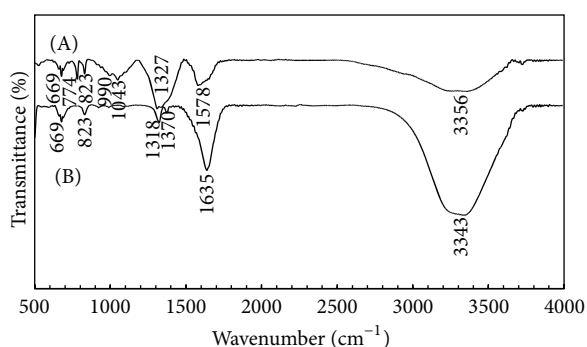


FIGURE 7: Infrared spectrum of aqueous extracts of *C. ambrosioides*. (A) Before bioreduction and (B) after bioreduction of silver ions.

plant, with a promising potential to produce a large amount of small particles (< 10 nm) in an ecofriendly protocol at 25°C with a proved stability after 368 days (one year) at 20°C.

It was demonstrated that varying the volume of reducing agent (leaf extract) and the molar concentration of AgNO₃ it is possible to control size and amount of nanoparticles. The -OH groups of terpenoids and flavonoids present in the leaf extracts are responsible for the reduction of silver ions and -COO groups participated in the stabilization of nanoparticles.

Conflict of Interests

The authors declare that there is no conflict of interests regarding the publication of this paper.

Acknowledgments

The authors thank Alejandra Núñez Pineda for technical assistance in IR characterization at the Laboratory of Thermal Analysis, Element and Infrared Analysis, of the “Centro Conjunto de Investigación en Química Sustentable, CCIQS, UAEM-UNAM” (Joint Center of Research in Sustainable

Chemistry), Mexico. The present research was granted by the “Fideicomiso Revocable y de Administración no. 157304 COLPOS” and the Línea de Investigación Prioritaria LPI-16 “Innovación Tecnológica” at the “Colegio de Postgraduados COLPOS” (Postgraduate College of Agriculture), Mexico.

References

- [1] L. Jia, Q. Zhang, Q. Li, and H. Song, “The biosynthesis of palladium nanoparticles by antioxidants in *Gardenia jasminoides* Ellis: long lifetime nanocatalysts for p-nitrotoluene hydrogenation,” *Nanotechnology*, vol. 20, no. 38, Article ID 385601, pp. 5601–5606, 2009.
- [2] L. Castro, M. Blázquez, J. A. Muñoz, F. González, C. García-Balboa, and A. Ballester, “Biosynthesis of gold nanowires using sugar beet pulp,” *Process Biochemistry*, vol. 46, no. 5, pp. 1076–1082, 2011.
- [3] V. Arya, “Living systems: eco-friendly nanofactories,” *Digest Journal of Nanomaterials and Biostructures*, vol. 5, no. 1, pp. 9–21, 2010.
- [4] S. Kaviya, J. Santhanalakshmi, B. Viswanathan, J. Muthumary, and K. Srinivasan, “Biosynthesis of silver nanoparticles using *Citrus sinensis* peel extract and its antibacterial activity,” *Spectrochimica Acta—Part A: Molecular and Biomolecular Spectroscopy*, vol. 79, no. 3, pp. 594–598, 2011.
- [5] R. G. Haverkamp and A. T. Marshall, “The mechanism of metal nanoparticle formation in plants: limits on accumulation,” *Journal of Nanoparticle Research*, vol. 11, no. 6, pp. 1453–1463, 2009.
- [6] A. T. Harris and R. Bali, “On the formation and extent of uptake of silver nanoparticles by live plants,” *Journal of Nanoparticle Research*, vol. 10, no. 4, pp. 691–695, 2008.
- [7] R. Bali, N. Razak, A. Lumb, and A. T. Harris, “The synthesis of metallic nanoparticles inside live plants,” in *Proceedings of the International Conference on Nanoscience and Nanotechnology (ICONN '06)*, pp. 224–227, July 2006.
- [8] A. Rico-Moctezuma, A. Vilchis-Néstor, V. Sánchez-Mendieta, M. Ávalos-Borja, and M. Camacho-López, “Biosíntesis de nanopartículas de oro mediante el extracto de *Opuntia ficus indica*,” *Superficies y Vacío*, vol. 23, supplement, pp. 94–97, 2010.
- [9] K. B. Narayanan and N. Sakthivel, “Coriander leaf mediated biosynthesis of gold nanoparticles,” *Materials Letters*, vol. 62, no. 30, pp. 4588–4590, 2008.
- [10] D. Philip, “Green synthesis of gold and silver nanoparticles using *Hibiscus rosa sinensis*,” *Physica E*, vol. 42, no. 5, pp. 1417–1424, 2010.
- [11] S. Li, Y. Shen, A. Xie et al., “Green synthesis of silver nanoparticles using *Capsicum annuum* L. extract,” *Green Chemistry*, vol. 9, no. 8, pp. 852–858, 2007.
- [12] N. Prabhu, D. T. Raj, K. Y. Gowri, S. A. Siddiqua, and D. J. P. Innocent, “Synthesis of silver phyto nanoparticles and their antibacterial efficacy,” *Digest Journal of Nanomaterials and Biostructures*, vol. 5, no. 1, pp. 185–189, 2010.
- [13] N. Ahmad, S. Sharma, M. K. Alam et al., “Rapid synthesis of silver nanoparticles using dried medicinal plant of basil,” *Colloids and Surfaces B: Biointerfaces*, vol. 81, no. 1, pp. 81–86, 2010.
- [14] A. D. Dwivedi and K. Gopal, “Biosynthesis of silver and gold nanoparticles using *Chenopodium album* leaf extract,” *Colloids and Surfaces A: Physicochemical and Engineering Aspects*, vol. 369, no. 1–3, pp. 27–33, 2010.

- [15] V. Armendariz, I. Herrera, J. R. Peralta-Videa et al., "Size controlled gold nanoparticle formation by *Avena sativa* biomass: use of plants in nanobiotechnology," *Journal of Nanoparticle Research*, vol. 6, no. 4, pp. 377–382, 2004.
- [16] P. Rajasekharreddy, P. U. Rani, and B. Sreedhar, "Qualitative assessment of silver and gold nanoparticle synthesis in various plants: a photobiological approach," *Journal of Nanoparticle Research*, vol. 12, no. 5, pp. 1711–1721, 2010.
- [17] Z. Kokanova-Nedialkova, P. T. Nedialkov, and S. D. Nikolov, "The genus *Chenopodium*: phytochemistry, ethnopharmacology and pharmacology," *Pharmacognosy Reviews*, vol. 3, no. 6, pp. 280–306, 2009.
- [18] F. R. F. Nascimento, G. V. B. Cruz, P. V. S. Pereira et al., "Ascitic and solid Ehrlich tumor inhibition by *Chenopodium ambrosioides* L. treatment," *Life Sciences*, vol. 78, no. 22, pp. 2650–2653, 2006.
- [19] S. P. Chandran, M. Chaudhary, R. Pasricha, A. Ahmad, and M. Sastry, "Synthesis of gold nanotriangles and silver nanoparticles using *Aloe vera* plant extract," *Biotechnology Progress*, vol. 22, no. 2, pp. 577–583, 2006.
- [20] J. Huang, Q. Li, D. Sun et al., "Biosynthesis of silver and gold nanoparticles by novel sundried *Cinnamomum camphora* leaf," *Nanotechnology*, vol. 18, no. 10, Article ID 105104, 2007.
- [21] M. Sathishkumar, K. Sneha, S. W. Won, C.-W. Cho, S. Kim, and Y.-S. Yun, "Cinnamon *zeylanicum* bark extract and powder mediated green synthesis of nano-crystalline silver particles and its bactericidal activity," *Colloids and Surfaces B: Biointerfaces*, vol. 73, no. 2, pp. 332–338, 2009.
- [22] J. Y. Song and B. S. Kim, "Rapid biological synthesis of silver nanoparticles using plant leaf extracts," *Bioprocess and Biosystems Engineering*, vol. 32, no. 1, pp. 79–84, 2009.
- [23] D. Cruz, M. Rodríguez, J. M. López, V. M. Herrera, A. O. Orive, and A. H. Creus, "Metallic nanoparticles and surface plasmons: a deep relationship," *Avances en Ciencias e Ingeniería*, vol. 3, no. 2, pp. 67–78, 2012.



Hindawi

Submit your manuscripts at
<http://www.hindawi.com>

